

Progress toward a Rationally Designed Molecular Motor†

T. ROSS KELLY

*Eugene F. Merkert Chemistry Center,
Department of Chemistry, Boston College,
Chestnut Hill, Massachusetts 02467*

Received September 26, 2000

ABSTRACT

A retrospective overview of the work in the author's laboratory leading to a prototype (**43a**) of a chemically powered molecular motor is provided. Beginning with a molecular brake (**23**) and then proceeding through a molecular "ratchet" (**31**), the development of a rationally designed molecular motor is described. The thermodynamic underpinnings of the concept are outlined, the synthetic routes to **23**, **31**, and **43a**, are summarized, and the data documenting the function of **23**, **31**, and **43a** are presented.

There is something about motors and other engines of motion (e.g., rockets, jets, steam engines, etc.) that particularly fascinates people. The aim of this Account is to recount our efforts to achieve the first rationally designed, chemically powered molecular motor. The task is still far from complete, but enough has now been accomplished to warrant a report on a work in progress.

The goal of achieving a molecular motor designed and constructed "from scratch" has been one of long duration, but for many years we were unable to conceive of a viable design. Thinking yet again about the challenge in 1993—and coming up, as usual, with no solution—it occurred to us that if we could not achieve a design for something that created movement, perhaps if we were able to accomplish something which stopped movement—a molecular brake^{1,2}—that might then provide insights which would ultimately help in the design of a molecular motor.

A Molecular Brake. The attempt to devise a molecular brake was our first foray into developing molecular devices, but it was not our first effort in molecular design.

T. Ross Kelly was born in 1942 and grew up in what was then the small town of Davis, CA. His interest in chemistry was first stimulated by a Gilbert Chemistry Set (which in those days contained powdered magnesium and other good things) and was nurtured in 1959 by a summer-long science program for high school students at the Loomis School in Connecticut sponsored by NSF (stimulated by the Soviet launch of Sputnik in 1957). He received a B.S. in chemistry (honors) from College of the Holy Cross in 1964, where he was turned on to organic chemistry by Professor Paul D. McMaster, and a Ph.D. from the University of California, Berkeley, where he carried out sesquiterpene total synthesis as Clayton H. Heathcock's first graduate student. After an NIH Postdoctoral Fellowship with James B. Hendrickson at Brandeis University, Kelly joined the faculty at Boston College in 1969, where he rose through the ranks and was named Vanderslice Professor of Chemistry in 1989. In 1982–1983, Kelly spent nine months on sabbatical at Pfizer, in Groton, CT, partly with the goal of learning how medicinal chemists designed molecules. Among the awards Kelly has received are an NIH Career Development Award (1975–1980) and an Arthur C. Cope Scholar Award (1996). It is perhaps relevant to the topic of this Account that Kelly has a shop in his home basement where he designs and builds furniture and other macroscopic constructions.

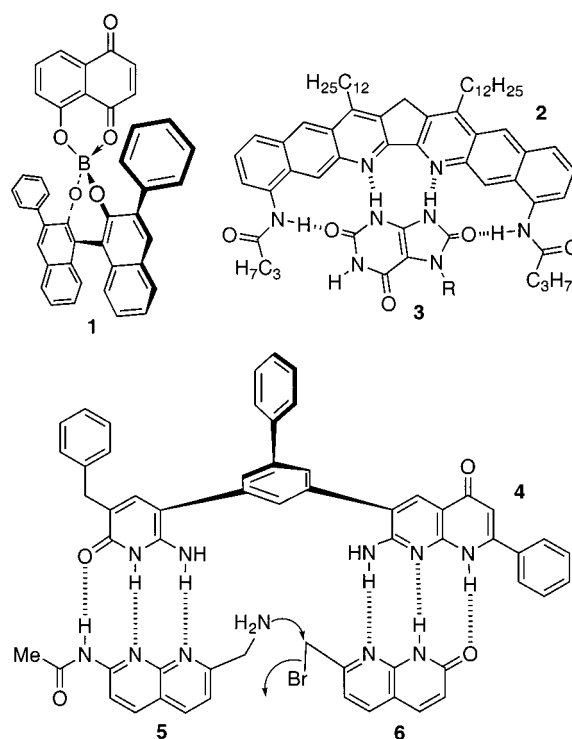


FIGURE 1. Earlier efforts in molecular design: **1**, a template for the asymmetric induction of Diels–Alder reactions; **2**, a receptor for uric acid-type molecules (**3**); **4**, a bisubstrate reaction template for promoting reactions between substrates **5** and **6**.

Earlier efforts (see Figure 1) resulting in a chiral Lewis acid for promoting asymmetric Diels–Alder reactions,³ a receptor for uric acid-type molecules,⁴ and a bisubstrate reaction template⁵ had taught us much about molecular design. In particular, we had learned some of what one could believe about space-filling models, and where a healthy skepticism remained warranted.⁶

Figure 2a shows a schematic design for our molecular brake. It consists of two parts: a three-toothed gear (the darker component) and a second unit shown in lighter color which could be remotely activated, inserting a "brake shoe" between the teeth of what was a normally spinning gear, thereby bringing rotation to a halt. The concept is much like the idea of sticking a broomstick into the spokes of a spinning bicycle wheel. Figure 2b depicts our original molecular embodiment (**7** → **8**) of the schematic in Figure 2a, where a triptycene functions as the spinning gear and is attached to the rest of the system by an acetylenic axle. Ordinarily the triptycene rotates rapidly around the axle, but it was hoped that braking action could be achieved by metal ion binding. The inclusion in the system of a bipyridine unit was anticipated to create braking action upon addition of a metal ion, because coordination of the two pyridine nitrogens to the metal ion forces the tricyclic brake shoe between the teeth of the triptycene. We hoped

† Part of the Special Issue on Molecular Machines.

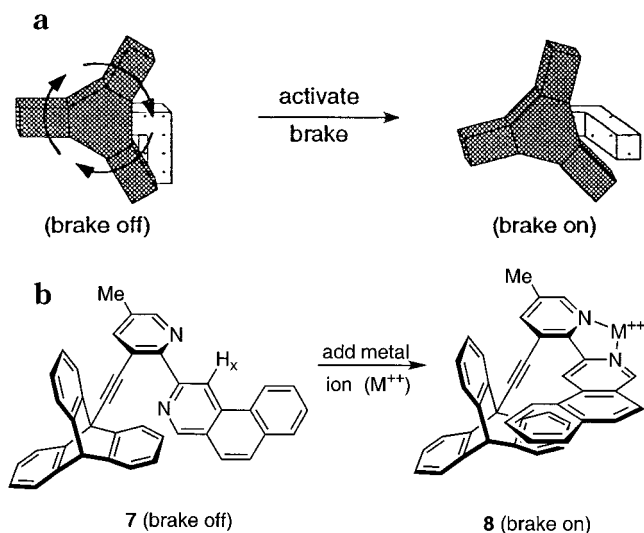
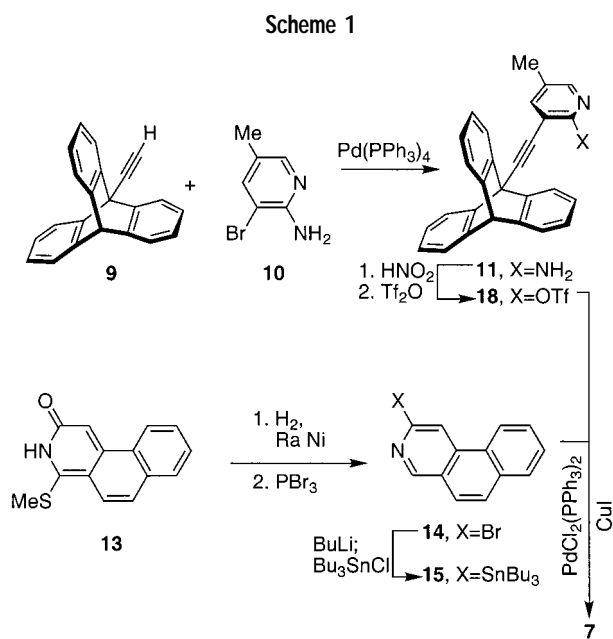


FIGURE 2. (a) Conceptual depiction of the operation of a molecular brake. (b) Original molecule designed to function as a molecular brake.

that such an action would bring the rotating triptycene to a halt.

Given the foregoing as the basis of the design, we turned to the synthesis of **7**, which is outlined in Scheme 1. The synthesis of **7** was tackled as a group project, and the first synthesis was actually accomplished in 13 days.



Addition of a variety of metal ions to solutions of **7** resulted in profound changes in the ¹H NMR spectrum, in agreement with the formation of a metal complex with a geometry resembling that shown in **8**. In particular, the peak in the NMR spectrum for H_x shifted nearly 2 ppm downfield, consistent with its being forced deep into the π cloud of the triple bond. Unfortunately, however, regardless of the metal ion used, the NMR spectrum indicated that the three blades of the triptycene were

equivalent, meaning that rotation was still rapid, even at temperatures as low as -110 °C.

In seeking to account for the failure of braking observed with **7/8**, we came to the conclusion that although the molecule did exist most of the time in the structure implicit in **8**, the acetylene was not sufficiently rigid. Thus, instead of inserting a broomstick through the bicycle wheel spokes, we were, in effect, replacing the broomstick with playing cards (as some children do with their bicycles, because they like the sound it makes), with the moving spokes repeatedly dislodging the playing cards.

The cure appeared to be to excise the acetylene and attach the pyridine directly to the triptycene, as shown in **16**. It was at this point that our prior work

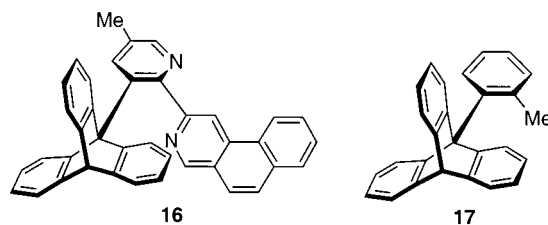
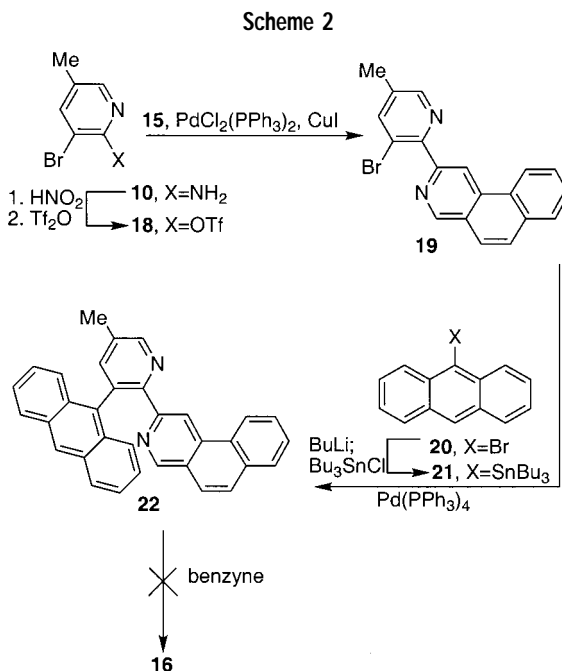
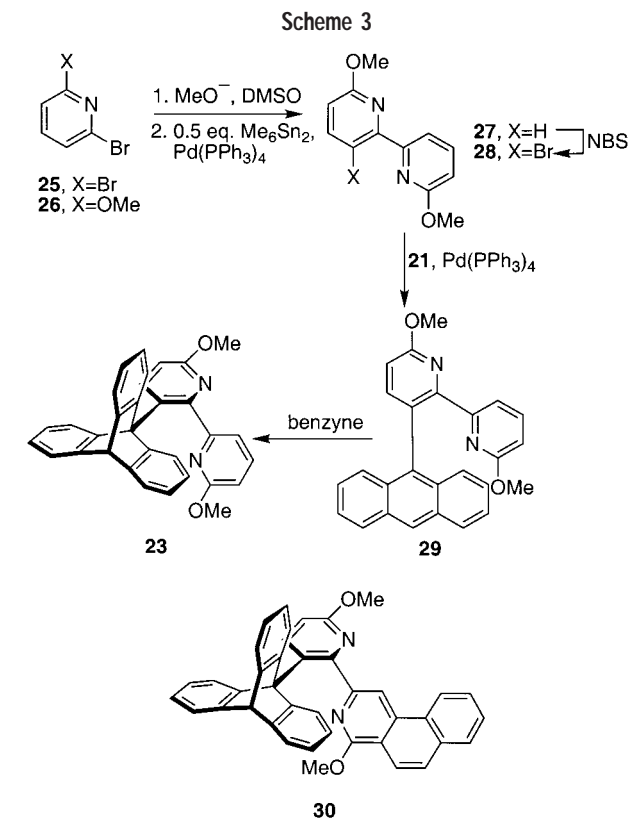


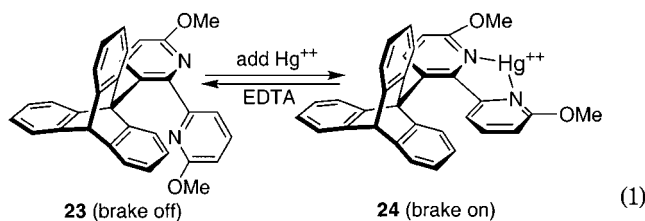
(Figure 1) in designing molecules paid dividends, because it is not possible to make space-filling (CPK) models of **16**. Nonetheless, we believed that the models were misleading, especially since compound **17** had been reported in the literature⁷ and seemed to have normal stability.



Unfortunately, the synthesis of **16** (Scheme 2) failed in the final step, the benzyne addition to **22**, for reasons we attribute to the electron-withdrawing properties of the pyridine on the anthracene. In the course of troubleshooting the synthesis of **16**, **23** was prepared as summarized in Scheme 3. We had intended to eventually modify a molecule such as **23** in order to incorporate a tricyclic brake shoe, as in **30**, but that proved unnecessary since **23** functioned as a molecular brake.



^1H NMR spectra of **23** (Figure 3) at room temperature indicate that the triptycene is spinning rapidly. Addition of mercuric ion to **23** engages the brake (eq 1) and slows



the rotation of the triptycene. At $-30\text{ }^\circ\text{C}$ the ^1H NMR spectrum (Figure 4) indicates that rotation is completely stopped on the NMR time scale. The NMR spectrum also shows that the brake is operating by the intended mechanism, because in its arrested state (**24**) the molecule has a plane of symmetry evidenced by a two-proton doublet for the two H_a protons and a one-proton doublet for the $\text{H}_{a'}$ proton. As the $-30\text{ }^\circ\text{C}$ sample is allowed to warm to $0\text{ }^\circ\text{C}$, the brake begins to slip, as indicated by the broadened peaks for H_a and $\text{H}_{a'}$. At room temperature the brake is slipping sufficiently that the peaks for H_a and $\text{H}_{a'}$ coalesce. Engagement of the brake can be reversed simply by addition of EDTA, which removes the mercuric ion, thereby converting **24** to **23**.

Our success in realizing the first molecular brake invigorated our quest for a molecular motor. But even though we had gleaned much from our efforts to achieve a molecular brake, we still had not learned how to construct a molecular motor. We had, however, reached the conclusion that it was likely that a necessary component of a molecular motor would be a ratchet.

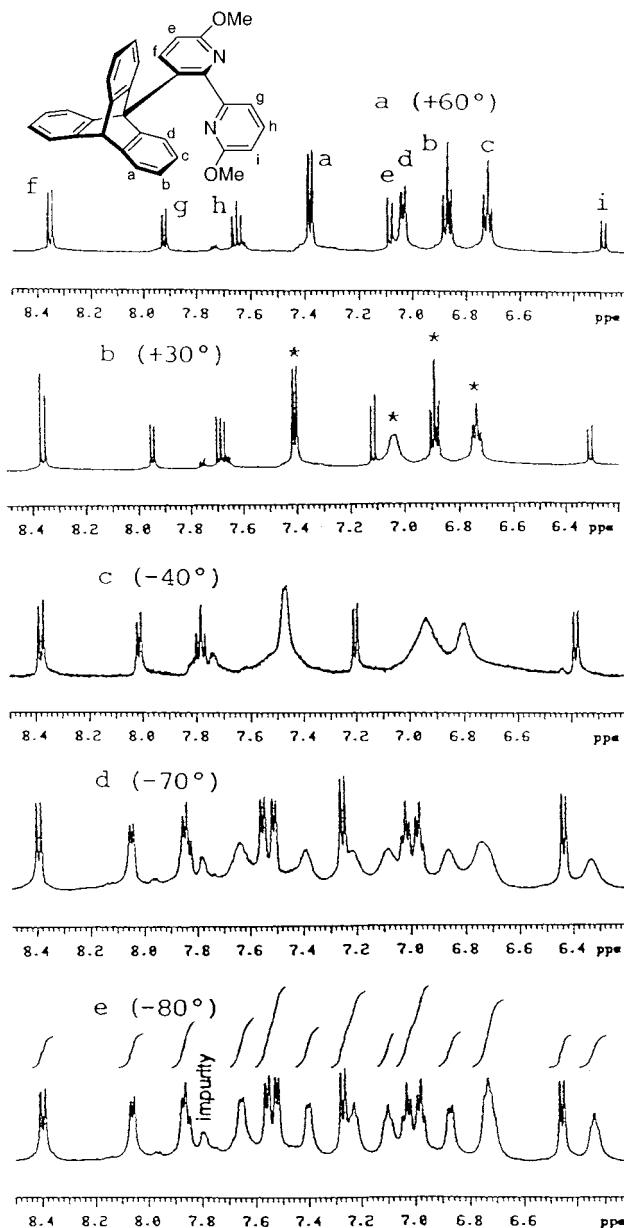


FIGURE 3. Aromatic region of the 500-MHz ^1H NMR spectrum (acetone- d_6) of **23** at various temperatures. Note that at $30\text{ }^\circ\text{C}$, the asterisked peaks for the 12 triptycene aromatic protons appear as four sets of resonances, indicating equivalence (due to relatively rapid rotation). At $-40\text{ }^\circ\text{C}$, peak broadening reflects slowed rotation, but even at $-70\text{ }^\circ\text{C}$, the broadened peaks indicate that rotation has not stopped on the NMR time scale. The sharp peaks in the $-80\text{ }^\circ\text{C}$ spectrum indicate that rotation has stopped, but not by engagement of a brake as in **24** [because the nonequivalence of all 12 triptycene protons in spectrum e indicates the absence of a plane of symmetry that is present in **24** (see text)].

A Molecular Ratchet.^{8–10} A schematic of a ratchet is shown in Figure 5. The three essential components of a ratchet are a wheel, a pawl, and a spring that holds the pawl against the wheel. In designing what we intended to be the ratchet, we retained the triptycene as the wheel, but switched the other component to a helicene, which we hoped would simultaneously serve as both the pawl and the spring. Although helicenes are helical rather than

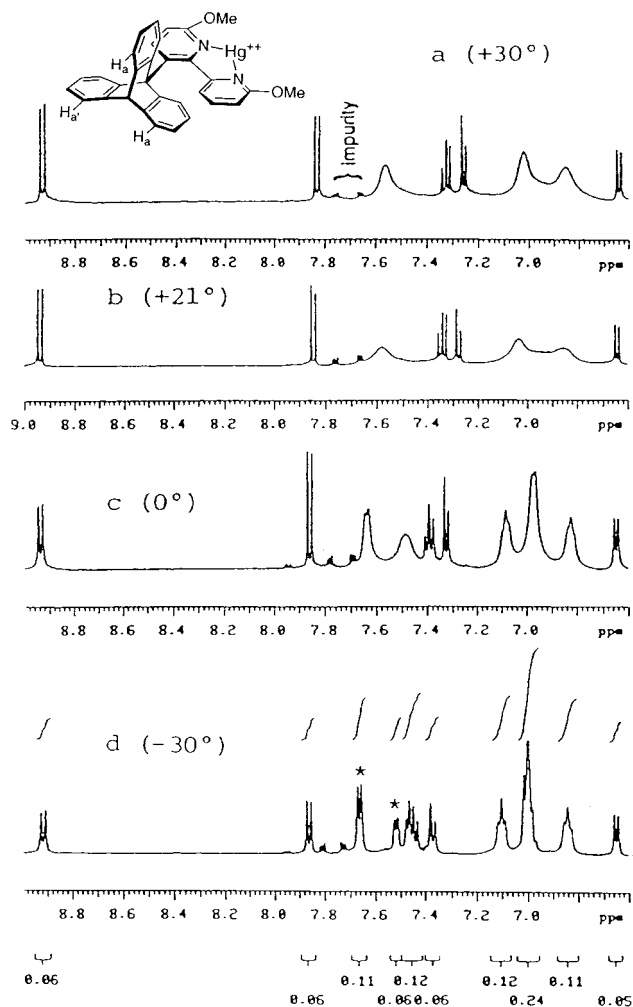
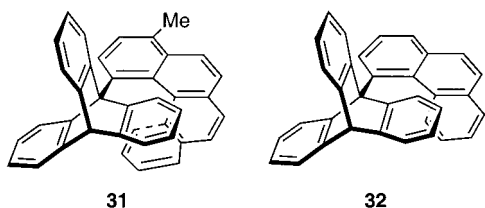


FIGURE 4. Aromatic region of the 500-MHz ^1H NMR spectrum (acetone- d_6) of **24**. Contrast the broad peaks at 30 °C with the sharp peaks at 30 °C in Figure 3b and the sharp peaks at -30 °C in this figure (indicating frozen rotation) with the broad peaks at -40 °C and -70 °C in Figure 3. The asterisked peaks in spectrum d correspond to the two equivalent H_a protons (on the left) and the one H_a' proton. Heating of the complex (**24**, $\text{M} = \text{Hg}^{2+}$) led to irreversible decomposition at ~ 70 °C before the spectrum had sharpened to reflect rapid triptycene rotation.

flat, we envisioned that rotation of the triptycene around the triptycene/helicene bond would twist the helicene more out of planarity than optimal, and resistance to that deformation would provide the restoring force inherent in a spring. The molecule we chose as the ratchet is **31** (the methyl group is included only for synthetic reasons). A stereoview of **3** is shown in Figure 6.



As a control, we elected also to prepare the [3]helicene derivative **32**. Molecular modeling¹¹ of the barrier to

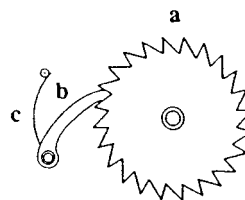


FIGURE 5. Simple mechanical ratchet: (a) ratchet wheel; (b) pawl; (c) spring that holds the pawl against the wheel.

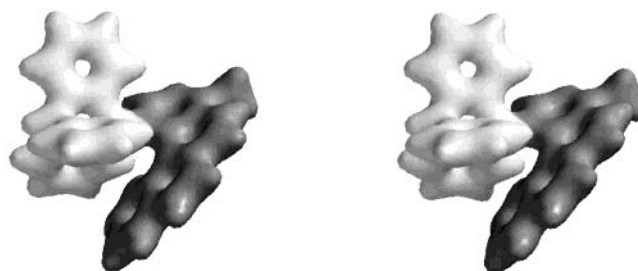
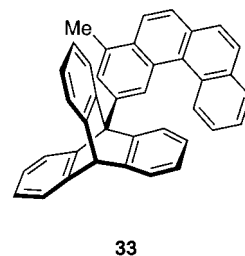
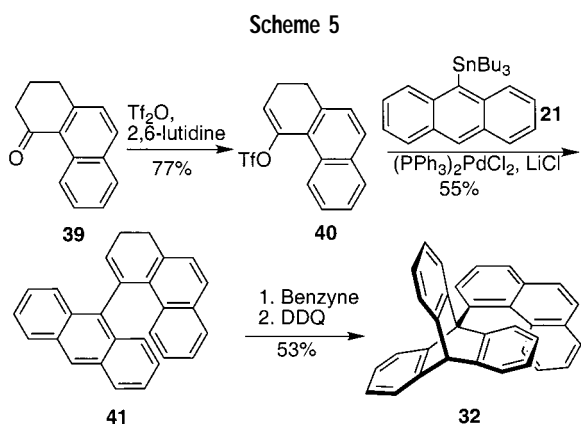
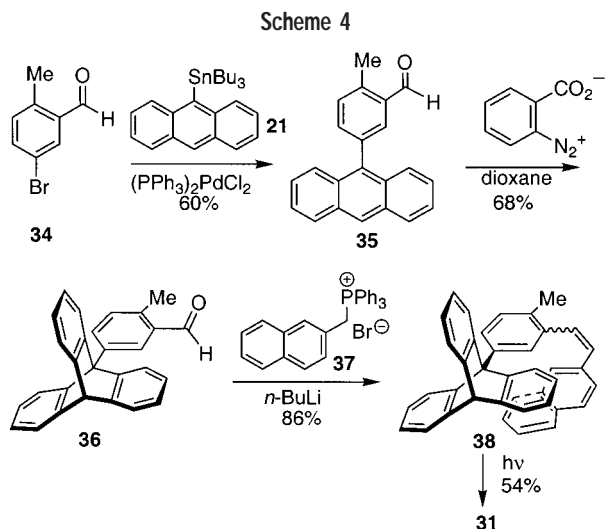


FIGURE 6. Stereoview of a calculated (AM1) electron density surface map of the lowest energy conformation of **31**. The triptycene rotor is in lighter tones, the helicene stator in darker tones. The calculated barrier to rotation ($\Delta H^\ddagger = 22$ kcal/mol) around the triptycene/helicene bond in **31** is in good agreement with the experimentally determined value ($\Delta G^\ddagger = 25$ kcal/mol).

rotation around the helicene/triptycene bond in **32** indicated, to our surprise, that the barrier to rotation in the [3]helicene was approximately 5 kcal/mol higher than the barrier to rotation in the [4]helicene **31**. To us, this finding was counterintuitive, since we expected the molecule with the bigger pawl to have the higher barrier to rotation. Since at that time we were not yet believers in molecular modeling (this project has made us become so), the unexpected modeling results were not troubling, because we did not trust them. As it turns out, however, the calculations proved correct. (One of the aspects of this work that has been most enjoyable is that we keep getting surprised by counterintuitive—to us—findings.) In retrospect, we attribute the higher barrier to rotation in **32** to the ability of the [3]helicene to drop lower into the space between the triptycene blades in **32**; in contrast, in **31** the [4]helicene gets “hung up” on a triptycene blade even in the most stable conformation and, as a result, the most stable ground state available is still destabilized. That conclusion is supported by the finding that, computationally, the most stable conformer of **31** is 14 kcal/mol less stable than its regioisomer **33**.



In due course, molecules **31** and **32** were synthesized by the routes indicated in Schemes 4 and 5. ^1H NMR



spectra of **31** and **32** were very revealing. In both cases the spectra indicated that at room temperature rotation around the triptycene/helicene bond was frozen on the NMR time scale. The NMR spectrum of **32** also showed the presence of a plane of symmetry, reminiscent of **24**, indicating that either the [3]helicene (phenanthrene) was planar or it existed as rapidly interconverting helicene enantiomers and, therefore, was incapable of functioning as a ratchet. In contrast, however, in the case of triptycyl[4]helicene **31**, ^1H NMR spectroscopy indicated that each of the three triptycene blades resided in a different environment. In other words, **31** appeared to have the potential to function as a ratchet. The calculated energy diagram (Figure 7) for rotation around the triptycene/helicene bond in **31** reinforced that expectation because of the curve's substantial asymmetry.

Two questions remained: (i) In which direction does the triptycene rotate? (ii) How does one tell?

Presumably, one could use isotopic labeling to determine the direction of rotation, but such a strategy would require a large investment of effort in synthesis, atropisomer separation, and structure assignment. The NMR technique of "spin polarization transfer", which allows one to "magnetically" label atoms, provides a much simpler method for answering the question. The peaks

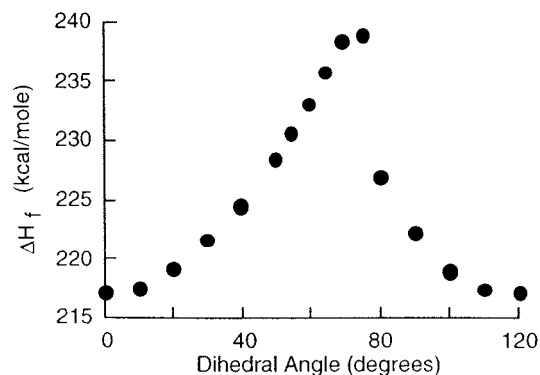
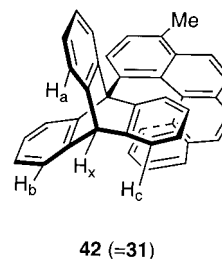


FIGURE 7. Calculated (AM1) energetics for clockwise rotation around the triptycene/[4]helicene bond in **31** (H instead of Me). Clockwise rotation of the triptycene corresponds to a left-to-right progression on the x axis.



corresponding to H_a , H_b , and H_c (see **42**) were identified using NOE correlations with the bridgehead proton, H_x , which was identified by its unique chemical shift. Because of the high barrier to rotation (which turns out to be 25 kcal/mol), we had to conduct the spin polarization experiments at 160 °C which, coincidentally, was the upper limit of our variable-temperature NMR probe.

The results of the spin polarization experiments are summarized in Figure 8 (which is, technically, a difference spectrum). Irradiation of the resonance for H_a (equivalent results were obtained in separate experiments irradiating H_b and, again separately, H_c) gave the spectra shown. If one performs an "observe" after a short delay, most of the polarization remains in the peak where it was originally put, but to the extent that any of the polarization has moved, it moves equally to the other two peaks. With longer delays before observing, more and more of the polarization moves, but it always moves equally to both other peaks. That is, the triptycene is rotating equally in both directions, and **31** is not functioning as a ratchet.

To those with a heightened sensitivity to the Second Law of Thermodynamics and the Principle of Microscopic Reversibility, that finding will come as no surprise. But to those who were seduced (manipulation of molecular models is particularly effective in this regard) into expecting unidirectional rotation, further explanation is perhaps in order. Reexamination of the energy diagram in Figure 7 is particularly informative. The asymmetry of the curve was noted earlier, but that is a red herring. What is more important is that, because of the symmetry of the triptycene, the energies of the two conformations designated 0° and 120° are identical. As anyone who has taken

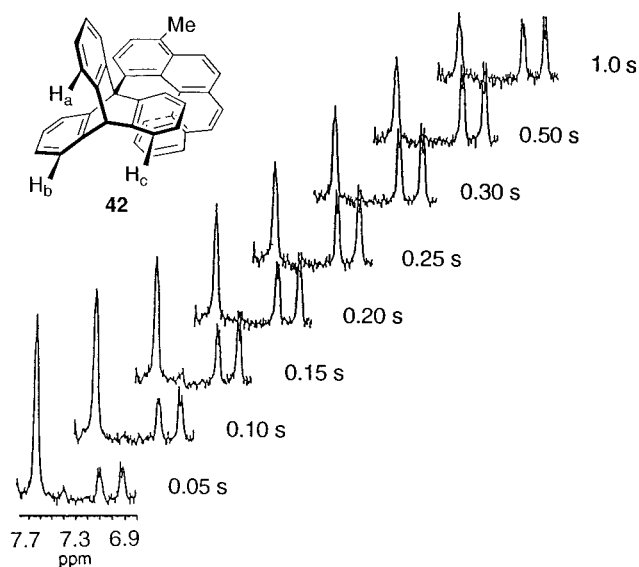


FIGURE 8. Results of spin polarization transfer experiment at 160 °C (calibrated temperature). The resonances for H_a , H_b , and H_c (see **42**) appear at δ 7.6, 7.1, and 6.9 ppm (not necessarily respectively). The spin of the proton resonating at δ 7.6 was polarized, and transfer of that polarization was monitored over time (the polarization stays with the proton originally polarized but, because of rotation, appears in a different peak).

(or taught) Introductory Organic Chemistry should remember, what is most important about an energy diagram is not the shape, but the height of the energy of activation hill. Since the energies at 0° and 120° in Figure 7 are identical, the barrier to rotation from 120° to 0° is

identical to the barrier for rotation from 0° to 120°. In other words, the barriers to clockwise and counterclockwise rotation are the same, and **31** could never have functioned as a ratchet.

So the question then becomes: How does one modify **31** to achieve unidirectional rotation; to wit, the motor?

A Prototype of a Molecular Motor.^{12,13} The concept is outlined in Figure 9, which is a partial reiteration of the energy diagram in Figure 7, except that it represents 240° of rotation around the triptycene/helicene bond, instead of only 120°, as in Figure 7. The black circle represents the energy of an individual molecule, with respect to rotation around the triptycene/helicene bond. As indicated in Figure 9b, most of the time the molecule is in a low-energy conformational state. Every once in a while, however, each molecule achieves a somewhat excited state with respect to rotation around the triptycene/helicene bond (the $t_{1/2}$ for thermally exciting molecules 10 kcal/mol above ground state at 25 °C is 2.3×10^{-6} s).¹⁴ If one can trap the molecule in the excited state c, figuratively by enlisting the brick wall shown in d then, to use a mountain-climbing analogy, in d the molecule is in a new base camp, closer to the energy of activation summit. Random thermal energy will then eventually elevate the molecule to the summit (e), from which it can descend the other side (\rightarrow f), which corresponds to unidirectional rotation from b to f. Put another way, once b has been trapped as in d, if one regards the right-hand half of panel d in Figure 9 as a new energy diagram where the black circle corresponds to the starting material, then that is

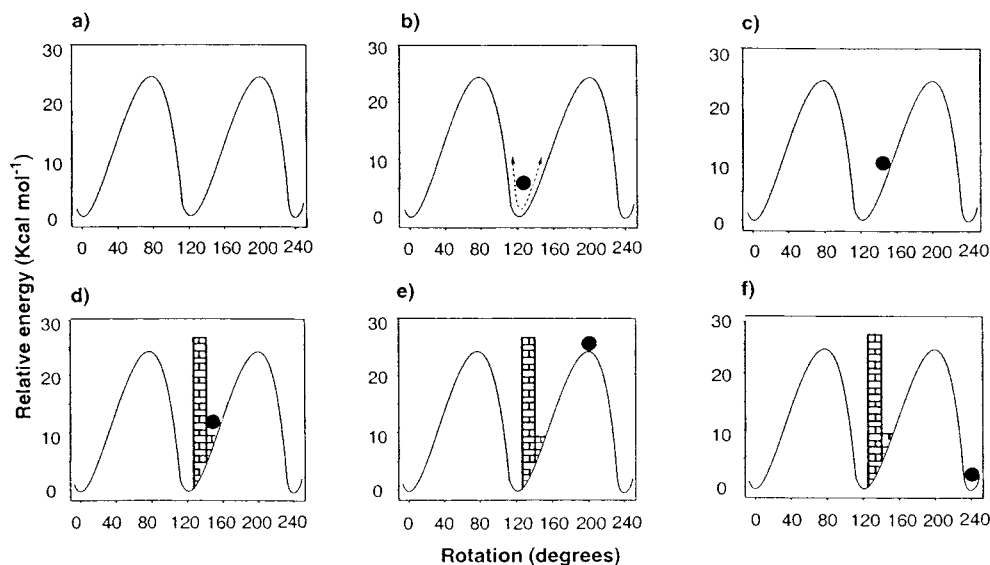


FIGURE 9. Schematic representation of the concepts underlying the design of the system. (a) Energy diagram representing 240° of rotation around the triptycene/helicene bond (black wedge in **31**), with a barrier of ~ 25 kcal/mol. (b) At any given time a single molecule (represented by the filled black circle) will usually exist in a low-energy conformation such as $\sim 120^\circ$ ($\approx 0^\circ$ and $\sim 240^\circ$ because of the three-fold symmetry of the triptycene) around the triptycene/helicene bond. (c) Within a very brief time span, random thermal energy temporarily elevates all individual molecules to conformationally excited states (for example, $t_{1/2}$ for thermally exciting molecules 10 kcal/mol above ground state at 25 °C is 2.3×10^{-6} s). (d) Conformationally excited rotamers in c are trapped and prevented from rotating back to a lower-energy conformation. (e) The trapped molecules are propelled by random thermal energy to the top of the energy barrier (reversion to the position in d—but not b—is possible, but readily reversible). (f) Descent from the summit in e to the next energy minimum is easy and virtually irreversible [because the reverse reaction (f \rightarrow e) has an energy requirement of +25 kcal/mol, which is effectively inaccessible ($t_{1/2}$ for achieving +25 kcal/mol is 63.2 h at 25 °C)].

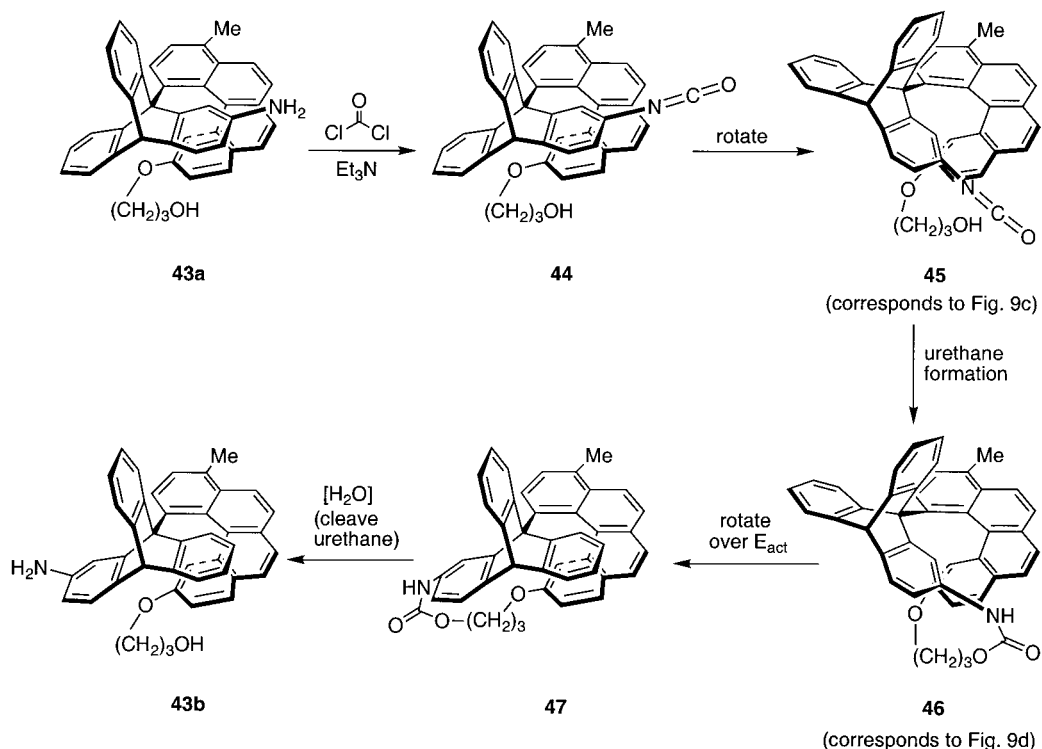
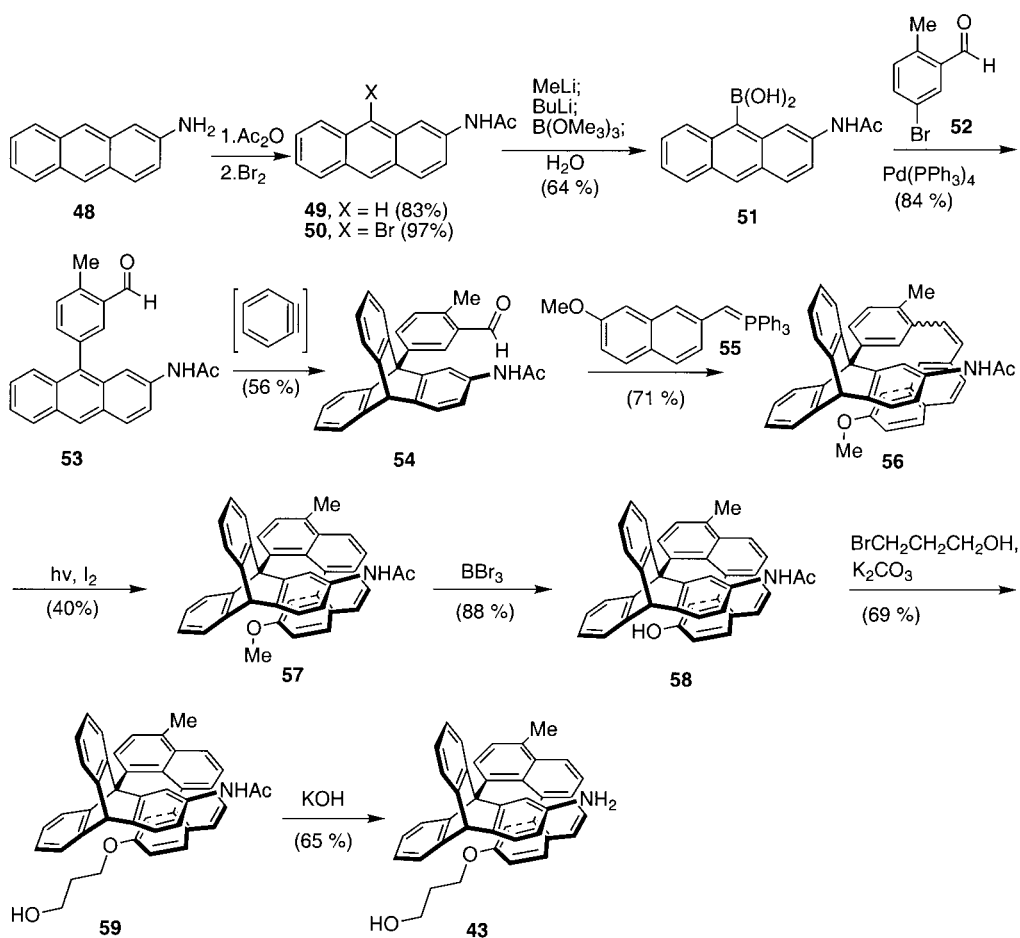


FIGURE 10. Sequence of events in the chemically powered rotation of **43a** to **43b**. See text for discussion. Although **43a** and **44** are not identical, to a first approximation they both conceptually correspond to Figure 9b. Compounds **45** and **46** correspond to Figure 9c and Figure 9d, respectively; compounds **47** and **43b** both correspond roughly to Figure 9f.

Scheme 6



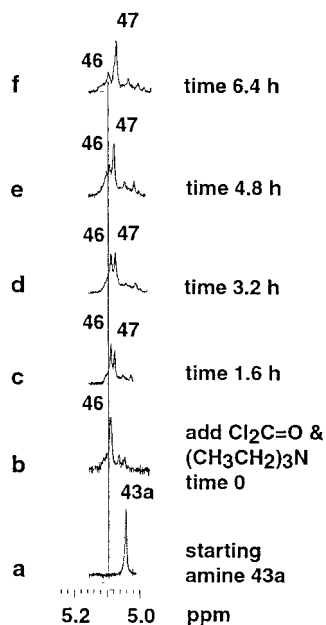


FIGURE 11. Spectroscopic evidence that phosgene fuels the unidirectional rotation of **43a**. Partial ^1H NMR spectra (monitoring the bridgehead proton) indicate the sequence of events as a function of time. Numbers next to peaks in the spectra refer to structures in Figure 10. (a) **43a** in CDCl_3 . (b) t_0 ; add $\text{Cl}_2\text{C}=\text{O}$ and Et_3N ; **43a** is rapidly converted to intramolecular urethane **46** via isocyanate **44**; the isocyanates **44** and **45** convert to **46** too rapidly to be seen in the spectra. (c) After 1.6 h at ambient temperature ($\sim 22^\circ\text{C}$) $\sim 30\%$ of **46** has rotated “over the hump” (Figure 9, **d** \rightarrow **f**) to **47**. (d–f) Over further time, rotation of **46** to **47** continues, with unidirectional conversion of **46** to **47** $>80\%$ complete in ~ 6 h. Urethane **47** was isolated and shown to be identical to material prepared directly from amine rotamer **43b** by reaction with $\text{Cl}_2\text{C}=\text{O}/\text{Et}_3\text{N}$. Control experiments established that **47** does not convert to **46**; i.e., that the conversion of **46** \rightarrow **47** is unidirectional.

an energy diagram for an exoergic reaction leading to **f**. The 25 kcal/mol released in the **e** \rightarrow **f** conversion is immediately released to the system and is not directly available to drive the reverse reaction.

The issue then becomes how to build the brick wall and trap the molecule in an excited state. As a proof of principle, we chose to modify the “ratchet” **31** to **43a** as shown in Figure 10, where an amino group is attached to one blade of the triptycene and a hydroxyalkyl group is attached to the helicene. Using the chemical fuel phosgene (which, to our mind, is chemically quite reminiscent of Nature’s standard fuel, ATP), the amino group in **43a** is to be armed as an isocyanate (**44**). In its low-energy conformations, the isocyanate is too far away from the hydroxy group attached to the helicene for urethane formation to occur between the two groups. However, if the triptycene rotates some 60° clockwise as drawn (\rightarrow **45**) to a conformationally excited state, then the isocyanate is close enough to the hydroxy group for urethane formation to occur (\rightarrow **46**), thereby trapping the molecule in an energetically excited conformation around the triptycene/helicene bond. Compound **46** corresponds to panel **d** in Figure 9. In due course, random thermal energy will cause **46** to rotate “over the hump” (the hump corresponds to panel **e** in Figure 9) and down the other

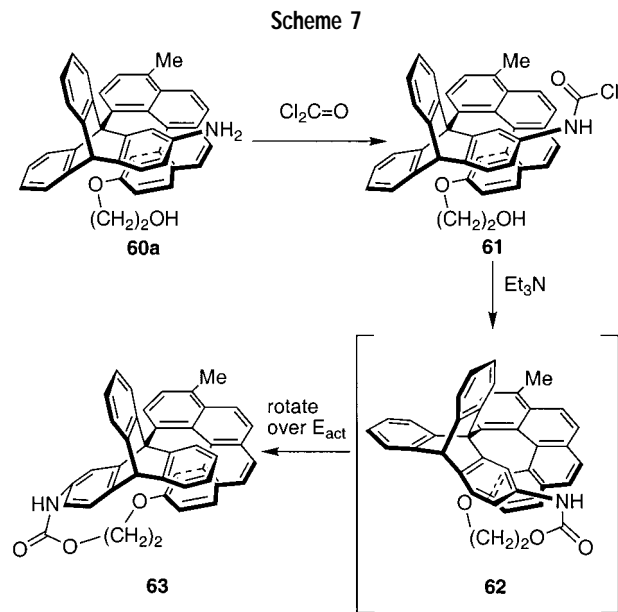
side to give **47**. Finally, cleavage of the urethane provides **43b**, in which the triptycene has rotated unidirectionally clockwise 120° . The design of **43** was worked out in part with molecular modeling (PM3) using the program Spartan.¹¹

The structure (**43**) chosen for the prototype was intentionally as similar to the structure of the “ratchet” **31** as possible, in order to make the best use of what had been learned earlier regarding synthesis and modeling. Nonetheless, the synthesis of **43**, which is summarized in Scheme 6, proved much more exacting than the synthesis of **31**. A multiyear synthetic effort did, however, ultimately provide **43**.

Once **43a** was in hand (and separated from its other two low-energy atropisomers), the time had arrived to experimentally evaluate the concepts. Using a combination of ^1H NMR (shown in Figure 11) and infrared (ReactIR technology;¹⁵ not shown) spectrometry to monitor reaction progress and assign structures, the essential concept was validated. In particular, addition of phosgene and Et_3N to a solution of **43a** in CDCl_3 resulted (Figure 10) in the **43a** \rightarrow **44** \rightarrow **45** \rightarrow **46** \rightarrow **47** conversion; Figure 11 provides the ^1H NMR data and the structures assigned to the individual peaks. Urethane **47** was then cleaved to **43b**. A control study demonstrated that reaction of atropisomer **43b** with $\text{Cl}_2\text{C}=\text{O}/\text{Et}_3\text{N}$ gave **47** but, importantly, **47** did not convert to **46**.

The chemically powered unidirectional rotation of **43a** to **43b** was thus achieved, and a prototype of a chemically powered molecular motor was in hand!

One additional study providing further support of the underlying strategic design has since been conducted. If the concepts illustrated in Figures 9 and 10 are valid, one should be able to accelerate the rate of rotation by shortening the tether attached to the helicene in **43a**, because then the truncated analogue will be trapped in a higher energy rotational state than **46**. In fact, that prediction is borne out. Replacement of the 3-carbon tether in **43a** with a 2-carbon tether as in **60a** (Scheme 7)



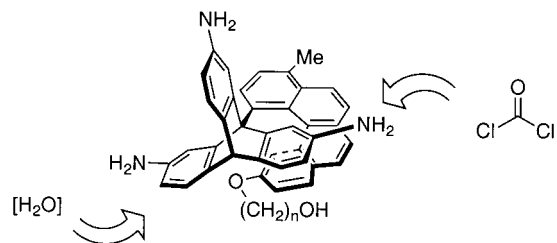


FIGURE 12. Schematic for a continually rotating molecular motor involving selective (and repeated) delivery of $\text{Cl}_2\text{C}=\text{O}$ to the amino group in the “firing” position and cleavage of the urethane only after each 120° of rotation has occurred.

not only results in faster rotation ($t_{1/2} \approx 5$ min instead of 3 h), but actually changes the rate-limiting step from **46** \rightarrow **47** in the case of the 3-carbon tether to **61** \rightarrow **62** in the case of the 2-carbon tether.

Conclusion. The results recounted above describe our efforts in the construction of molecular devices, beginning with a molecular brake and leading to the prototype of a chemically powered molecular motor. Much remains to be done before our motor rivals in speed and continual operation its biological and mechanical counterparts. The next step, however, is now clear: to achieve repeated rotation by modifying **43a/60a** so that each blade of the triptycene is ready to be selectively armed at the appropriate time, and to include in the system (e.g., by attachment to the helicene) units with the appropriate spatial positioning that can capture and deliver $\text{Cl}_2\text{C}=\text{O}$ and cleave a urethane, as represented in Figure 12. Efforts in that direction are now in progress. It is our hope that the work to date may also lead to a better understanding of some of the design features underlying biological and other molecular motors.

I express my deepest gratitude to the students and postdoctoral associates whose names appear as coauthors in the references for all that they achieved in converting wishful thinking into chemical reality. The National Institutes of Health is acknowledged for support of the work on the molecular motor (Grant GM56262); last, but far from least, we thank the MCHA Study Section for taking a chance on a high-risk proposal.

References

- (1) Kelly, T. R.; Bowyer, M. C.; Bhaskar, K. V.; Bebbington, D.; Garcia, A.; Lang, F.; Kim, M. H.; Jette, M. P. A Molecular Brake. *J. Am. Chem. Soc.* **1994**, *116*, 3657–3658. Note the Experimental Section in the Supplementary Material.
- (2) For reviews of molecular machines and devices, see: Mislow, K. Molecular Machinery in Organic Chemistry. *Chemtracts–Org. Chem.* **1989**, *2*, 151–174. Stoddart, J. F.; Balzani, V.; Credi, A.; Raymo, F. M. Toward Artificial Molecular Machines. *Angew. Chem., Int. Ed.* **2000**, *39*, 3348–3391. *Molecular Machines and Motors*; Sauvage, J.-P., Ed. *Struct. Bonding (Berlin)* **2001**, *99*.
- (3) Kelly, T. R.; Whiting, A.; Chandrakumar, N. S. A Rationally Designed, Chiral Lewis Acid for the Asymmetric Induction of Some Diels–Alder Reactions. *J. Am. Chem. Soc.* **1986**, *108*, 3510–3512.
- (4) Kelly, T. R.; Maguire, M. P. A Receptor for the Oriented Binding of Uric Acid Type Molecules. *J. Am. Chem. Soc.* **1987**, *109*, 6549–6951.
- (5) Kelly, T. R.; Zhao, C.; Bridger, G. J. A Bisubstrate Reaction Template. *J. Am. Chem. Soc.* **1989**, *111*, 3744–3745. Kelly, T. R.; Bridger, G. J.; Zhao, C. Bisubstrate Reaction Templates. Examination of the Consequences of Identical versus Different Binding Sites. *J. Am. Chem. Soc.* **1990**, *112*, 8024–8034.
- (6) Kelly, T. R.; Bilodeau, M. T.; Bridger, G. J.; Zhao, C. Receptors for Uric Acids. 2. A Cautionary Observation. *Tetrahedron Lett.* **1990**, *30*, 2485–2488.
- (7) Nakamura, M.; Oki, M. Restricted Rotation Involving the Tetrahedral Carbon. XV. Restricted Rotation about a $\text{Csp}^3\text{–Csp}^2$ Bond in 9-Aryltriptycene Derivatives. *Bull. Chem. Soc. Jpn.* **1975**, *48*, 2106–2111.
- (8) Kelly, T. R.; Tellitu, I.; Sestelo, J. P. In Search of Molecular Ratchets. *Angew. Chem., Int. Ed. Engl.* **1997**, *36*, 1866–1868. Kelly, T. R.; Sestelo, J. P.; Tellitu, I. New Molecular Devices: In Search of a Molecular Ratchet. *J. Org. Chem.* **1998**, *63*, 3655–3665.
- (9) Davis, A. P. Tilting at Windmills? The Second Law Survives. *Angew. Chem., Int. Ed.* **1998**, *37*, 909–910.
- (10) Musser, G. Taming Maxwell’s Demon. *Sci. Am.* **1999**, *280*, 24.
- (11) Spartan, Wavefunction, Inc., Irvine, CA. Version 4.0 (1995) for Silicon Graphics computers was used.
- (12) Kelly, T. R.; De Silva, H.; Silva, R. A. Unidirectional Rotary Motion in a Molecular System. *Nature* **1999**, *401*, 150–152. Kelly, T. R.; Silva, R. A.; De Silva, H.; Jasmin, S.; Zhao, Y. A Rationally Designed Prototype of a Molecular Motor. *J. Am. Chem. Soc.* **2000**, *122*, 6935–6949.
- (13) For a photochemically powered molecular motor, see: Koumura, N.; Zijlstra, R. W. J.; van Delden, R. A.; Harada, N.; Feringa, B. L. Light-Driven Monodirectional Molecular Rotor. *Nature* **1999**, *401*, 152–154.
- (14) Scudder, P. H. *Electron Flow in Organic Chemistry*; John Wiley & Sons: New York, 1992; p 40.
- (15) ASI Applied Systems, Millersville, MD 21109, USA. For a bibliography of applications, see www.asirxn.com.

AR000167X